arXiv:cond-mat/0601534v3 [cond-mat.soft] 27 Apr 2006

Direct Numerical Simulations of Electrophoresis of Charged Colloids

Kang Kim,[1,2] Yasuya Nakayama,[3,2] and Ryoichi Yamamoto[1,2]

[1] *Department of Chemical Engineering, Kyoto University, Kyoto 615-8510, Japan*
[2] *PRESTO, Japan Science and Technology Agency, Kawaguchi 332-0012, Japan*
[3] *Department of Chemical Engineering, Kyushu University, Fukuoka 819-0395, Japan*

We propose a numerical method to simulate electrohydrodynamic phenomena in charged colloidal dispersions. This method enables us to compute the time evolutions of colloidal particles, ions, and host fluids simultaneously by solving Newton, advection-diffusion, and Navier–Stokes equations so that the electrohydrodynamic couplings can be fully taken into account. The electrophoretic mobilities of charged spherical particles are calculated in several situations. The comparisons with approximation theories show quantitative agreements for dilute dispersions without any empirical parameters, however, our simulation predicts notable deviations in the case of dense dispersions.

PACS numbers: 82.70.Dd 47.65.-d 82.20.Wt 82.45.-h

Electrohydrodynamic phenomena are of great importance in physical, chemical, and biological science, and also in several engineering fields [1]. In the case of electrophoresis of charged particles for example, the particles start to move on the application of external electric fields. The electric double layer, *i.e.* the cloud of counterions around charged particles, tends to be deformed and its distribution becomes anisotropic because of the applied external field and also of the friction between ions and fluids. The electrophoretic mobility of a single colloidal particle is then determined by the balance between the electrostatic driving force and the hydrodynamic frictional force acting on the particle. In this situation, the time evolutions of the colloidal particles, the ions, and the host fluids are described by coupled equations of hydrodynamics (Navier-Stokes) and electrostatics (Poisson) with proper boundary conditions imposed on the surfaces of the colloidal particles. However, the usual numerical techniques of partial differential equations are hopeless to deal with dynamical evolutions of many-particle systems since the moving particle-fluid boundary condition must be treated at every discrete time step.

In late years, efforts to resolve hydrodynamic interactions in colloidal dispersions attract much attention. Various advanced methods have been proposed such as the Stokesian Dynamics (SD) [2], the finite element method (FEM) [3], the Lattice Boltzmann method (LBM) [4], the Stochastic Rotation Dynamics [5], the Fluid Particle Dynamics (FPD) [6], and yet another method which treats solid-fluid interaction efficiently [7]. Pioneering approaches have been proposed also to simulate charged colloidal dispersions without hydrodynamics [8, 9, 10, 11, 12]. Although extensions have been done to take into account the hydrodynamics by using SD [13], FEM [14], LBM [15, 16, 17, 18, 19], and FPD [20], quantitatively reliable simulations have not yet been performed successfully for many particle dispersions due to the complexity of the system.

Recently, we developed a reliable and efficient numerical method, called smoothed profile (SP) method [21, 22], to resolve the hydrodynamic interactions acting on solid particles immersed in Newtonian host fluids. In the SP method, the original sharp boundaries between colloids and host fluids are replaced with diffuse interfaces with finite thickness ξ. This simple modification greatly improve the performance of numerical computations since it enables us to use the fixed Cartesian grid even for the problems with moving boundary conditions.

The SP method is not only applicable to the dispersions in Newtonian fluids, but particularly suitable for the particle dispersions in complex fluids. It has already been applied successfully to liquid crystal colloidal dispersions [23, 24] and charged colloidal dispersions [25]. Field-particle hybrid simulations were performed, where the average direction of the liquid crystal molecules and the density of ions were treated as coarse-grained continuum objects while colloids were treated explicitly as particles. The interaction between fields and particles were taken through the diffuse interface. The above methods for the dispersions in complex fluids are, however, not yet appropriate for simulating dynamical phenomena since hydrodynamic effects are completely neglected. The purpose of the present study is to establish an efficient and reliable simulation method applicable for electrohydrodymanic phenomena such as electrophoresis by combining our SP methods for hydrodynamic [21, 22] and electrostatic [25] interactions.

In the present paper, we briefly outline our numerical modeling for charged colloidal dispersions and then demonstrate the reliability of the combined SP method by comparing our numerical results with classical approximation theories [26, 27, 28, 29]. Finally, comparisons are made for the electrophoretic mobilities of dense dispersions, where the simulation results show notable deviations from a mean-field type theory according to the cell model [30, 31].

Let us consider N spherical particles with radius a, the mass M_p, and the inertia tensor $\boldsymbol{I}_p$ in a host fluid consisting of multi-component ions of species α with charges $Z_\alpha e$, where e is the unit charge. The local number density

of α ion is $C_\alpha(\vec{r},t)$ at a time t. The total charge on a colloidal particle is Ze and distributed uniformly on its surface. The velocity field of the host fluid is $\vec{v}(\vec{r},t)$. The position, the translational velocity, and the angular velocity of the ith particle are $\vec{R}_i$, $\vec{V}_i$, and $\vec{\Omega}_i$, respectively. We define the overall profile function $\phi(\vec{r},t) \equiv \sum_{i=1}^{N} \phi_i(\vec{r},t)$, where $\phi_i \in [0,1]$ is the ith particle's profile field which is unity in the particle domain $|\vec{r}-\vec{R}_i| < a-\xi/2$, zero in the fluid domain $|\vec{r}-\vec{R}_i| > a+\xi/2$, and have a continuous diffuse interface within the thin interface domain $a-\xi/2 < |\vec{r}-\vec{R}_i| < a+\xi/2$ whose thickness is ξ. The mathematical definition of ϕ_i is given in Ref. [21]. We define the spacial distribution of the surface charge $eq(\vec{r}) = Ze|\nabla\phi|/4\pi a^2$ using ϕ, then the local density of the total charge is represented smoothly everywhere in the system by $\rho_e(\vec{r}) \equiv \sum_\alpha Z_\alpha e C_\alpha + eq$. The complete dynamics of the system is obtained by solving the following time evolution equations [21, 22].

i) The Navier–Stokes equation:

$$\rho(\partial_t + \vec{v}\cdot\nabla)\vec{v} = -\nabla p + \eta\nabla^2\vec{v} - \rho_e\nabla(\Psi+\Psi_{ex}) + \phi\vec{f}_p, \quad (1)$$

with incompressible condition $\nabla\cdot\vec{v}=0$, where ρ is the mass density, p is the pressure, η is the shear viscosity of the host fluid, $\Psi_{ex} = -\vec{E}\cdot\vec{r}$ is the external electric potential due to the constant electric field $\vec{E}$, and $\phi\vec{f}_p$ represents the body force arising from the rigidity of the particles [22]. The electrostatic potential $\Psi(\vec{r})$ is to be determined by solving the Poisson equation $\epsilon\nabla^2\Psi = -\rho_e$ with the dielectric constant ϵ of the host fluid.

ii) The Newton's and Euler's equations of motions:

$$\dot{\vec{R}}_i = \vec{V}_i, \quad M_p\dot{\vec{V}}_i = \vec{F}_i^H + \vec{F}_i^c, \quad \boldsymbol{I}_p\cdot\dot{\vec{\Omega}}_i = \vec{N}_i^H, \quad (2)$$

where $\vec{F}_i^H$ and $\vec{N}_i^H$ are the hydrodynamic force and torque [22], and $\vec{F}_i^c$ is the force arising from the excluded volume of particles which prevents colloids from overlapping. Hereafter, soft-core potential of the truncated Lennard–Jones potential is adopted for $\vec{F}_i^c$. We include the electric driving force due to $\vec{E}$ in $\vec{F}_i^H$.

iii) Advection-diffusion equation:

$$\partial_t C_\alpha^* = -\nabla\cdot C_\alpha^*\vec{v} + f_\alpha^{-1}\nabla\cdot((\boldsymbol{I}-\vec{n}\vec{n})\cdot C_\alpha^*\nabla\mu_\alpha), \quad (3)$$

where f_α is the ionic friction coefficient, $\boldsymbol{I}$ is the unit tensor, and $\vec{n}$ is a unit-vector field defined by $\vec{n} = -\nabla\phi/|\nabla\phi|$. In our method, the actual density fields of ions are defined as $C_\alpha(\vec{r},t) = (1-\phi(\vec{r},t))C_\alpha^*(\vec{r},t)$ using the auxiliary density field $C_\alpha^*(\vec{r},t)$. This definition avoids penetration of ions into colloids explicitly without using artificial potentials, which requires smaller time increments. The operator $(\boldsymbol{I}-\vec{n}\vec{n})$ in Eq.(3) ensures the conservation of C_α since the no-penetration condition, $\vec{n}\cdot\nabla\mu_\alpha = 0$ is directly assigned at the diffuse interface. Then the charge neutrality $\int \rho_e d\vec{r} = 0$ of the total system is guaranteed automatically. Based on the density functional theory [32, 33], the chemical potential is defined as

$$\mu_\alpha = k_BT\ln C_\alpha^* + Z_\alpha e(\Psi+\Psi_{ex}), \quad (4)$$

where k_B is the Boltzmann constant and T is the temperature. If we set $\vec{v}=0$ in Eq. (3), the equilibrium ($t\to\infty$) ionic density is given by the Boltzmann Eq.

$$C_\alpha^* = \bar{C}_\alpha \exp[-Z_\alpha e(\Psi+\Psi_{ex})/k_BT]. \quad (5)$$

The bulk salt concentration $\bar{C}_\alpha$ is related to the Debye screening length $\kappa^{-1} = 1/\sqrt{4\pi\lambda_B\sum_\alpha Z_\alpha^2\bar{C}_\alpha}$, where $\lambda_B = e^2/4\pi\epsilon k_BT$ is the Bjerrum length which is approximately 0.72nm in water at 25 °C.

Simulations have been performed in a three-dimensional cubic box with the periodic boundary conditions. The linear dimension is $L/\Delta = 64$, where Δ is the lattice spacing chosen as a unit length, which is taken related to the Bjerrum length as $\Delta = 4\pi\lambda_B$. We use the particle radius $a=5$ and the thickness parameter $\xi=2$ throughout the present simulations. The host fluid contains 1:1 electrolyte composed of monovalent counterions ($\alpha=+$) and coions ($\alpha=-$). The unit of the energy and the electrostatic potential is k_BT and k_BT/e, respectively. The later corresponds to 25.7mV at 25 °C. The non-dimensional parameter $m_\alpha = 2\epsilon k_BTf_\alpha/3\eta e^2$ is set to be $m_+ = m_- = 0.184$, which corresponds to the value of KCl solution at 25 °C. Our unit of time $\tau = \Delta^2 f_+/k_BT$ corresponds to 0.44μsec.

We first consider a single charged particle moving with the drift velocity $\vec{V} = (-V,0,0)$ in a constant electric field $\vec{E} = (E,0,0)$. The electrophoretic mobility V/E is

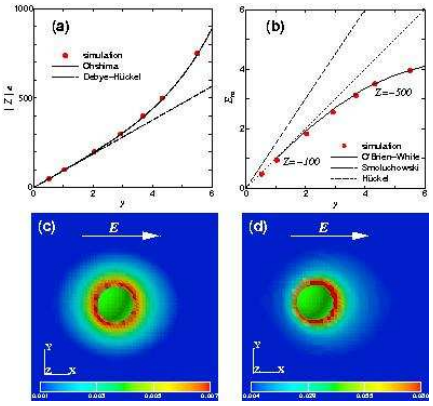

FIG. 1: Relationship between surface charge $|Z|e$ and dimensionless zeta potential y (a). Our numerical data follows nicely on the analytic solution of the nonlinear PB equation [34] but deviates notably from the Debye–Hückel linearized theory. Dimensionless mobility E_m of a single particle is plotted in (b) as a function of dimensionless zeta potential y. For comparison, results of Smolchowski, Henry, and O'Brien–White for $\kappa a = 0.5$ are plotted. The color contours in (c) and (d) represent the total ionic charge density $\sum_\alpha eZ_\alpha C_\alpha$ around a single particle for (c) $Z=-100$ and (d) $Z=-500$. The electric field is applied in the horizontal ($+x$) direction.

related to the zeta potential ζ, which is defined as the electrostatic potential on a slipping plane, as

$$V/E = f\epsilon\zeta/\eta \tag{6}$$

when ζ is small [1]. The Smolchowski equation $f = 1$ is valid in the limiting case $\kappa a \to \infty$ [27], while the Hückel equation $f = 2/3$ is valid in the opposite case $\kappa a \to 0$ [28]. Henry derived an expression $f = f_H(\kappa a)$ which is valid for a general value of κa [29]. These equations indicate that the mobility is proportional to ζ, however, this relation tends to fail for larger ζ where the relaxation effect due to deformations of electric double layer becomes notable. O'Brien and White proposed an approximation theory which is valid also for larger ζ [26].

We have performed simulations for electrophoresis of a single particle in linear response regimes $E \lesssim 0.15$ and compared them with the O'Brien–White theory. A constant uniform electric field $E = 0.1$, which corresponds to 2.85×10^3V/cm, was applied. The terminal V was calculated for $50 \le -Z \le 750$ with $\kappa^{-1} = 10$, corresponding to the salt concentration 11μmol/l at 25 °C in water. We chose $\nu = \eta/\rho = 5$, so the Reynolds number $Re = aV/\nu$ remains small. Both in the O'Brien–White theory and our simulations, the zeta potential is assumed to be the electrostatic potential at the particle surface, $\zeta = \Psi|_{\rm surface}$. In our simulations, the surface charges were chosen as $Z = -50$, -100, -200, -300, -400, -500, and -750, corresponding to $y = 0.525$, 1.044, 2.035, 2.927, 3.692, 4.332, and 5.510, respectively. Here the dimensionless zeta potential $y \equiv e\zeta/k_BT$ is introduced. A relationship between the surface charge $|Z|e$ and the dimensionless zeta potential y is shown in Fig.1(a), where our numerical results are plotted together with an analytic solution of the nonlinear PB equation [34] and the Debye–Hückel linearized solution $\zeta = |Z|e/4\pi a^2\epsilon\kappa(1 + \kappa a^{-1})$. We see that our numerical results are consistent with the nonlinear PB theory. In Fig.1(b), the dimensionless mobility $E_m \equiv 3e\eta V/2\epsilon k_BTE$ is plotted as a function of the dimensionless zeta potential with $\kappa a = 0.5$. It is clearly demonstrated that our method reproduced the O'Brien–White theory almost perfectly including the nonlinear regime $y \ge 2$ only within a few percent error. We emphasize that such a precise agreement with the theory has never been obtained by any simulation methods so far proposed. The distributions of charge density due to counterions and coions are shown in Fig.1(c) for $y = 1.044$ and (d) for $y = 3.692$. One can see that the electric double layer is deformed considerably in the nonlinear regime (d), while it is almost isotropic in the linear regime (c). As is mentioned before, the relaxation effect due to the deformed double layer causes the nonlinearity in E_m.

Our simulation method is easily applicable to dense dispersions consisting of many particles. We thus examined the effect of the particle concentration on the electrophoretic mobility. The linearized theory for a single particle Eq.(6) is still valid for dense dispersions when E is small, however, f is now depending both on κa and φ. Simulations were carried out with $Z = -100$ and $E = 0.1$ for various particle volume fractions $\varphi \equiv 4\pi a^3N/3L^3$ to calculate $f(\kappa a, \varphi) = \eta V/\epsilon\zeta E$. The Debye length κ^{-1} is taken to be 5 and 10 which correspond to $\kappa a = 1$ and 0.5, respectively. The corresponding salt concentration is 44μmol/l for $\kappa^{-1} = 5$ and 11μmol/l for $\kappa^{-1} = 10$, respectively. Figure 2 shows typical snapshots of the systems with (a) FCC, (b) BCC, and (c) random configurations [35]. The horizontal color map represents the charge density for $\kappa a = 1$ on a cross section perpendicular to z axis. In the cases of FCC and BCC, E was applied perpendicular to the (1,0,0) and (1,1,1) faces, but we obtained very small differences only within 1%.

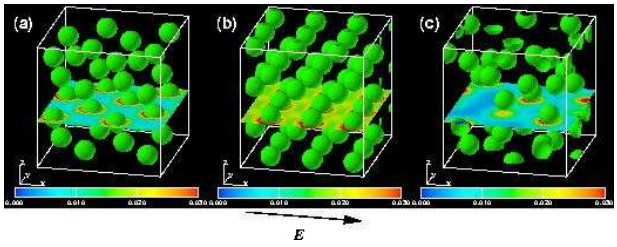

FIG. 2: Snapshots of the electrophoresis of dense dispersions with (a) FCC, (b) BCC, and (c) random particle configurations. The color map represents the total ionic charge density $\sum_\alpha eZ_\alpha C_\alpha$ in a plane perpendicular to z axis. The electric field is applied in $+x$ direction normal to (1,0,0) face for FCC and BCC. See movies [35].

The mobility coefficient $f(\kappa a, \varphi)$ for $\kappa a = 1$ and 0.5 is plotted as a function of φ in Fig. 3 (a) and (b), respectively. We found that f decreases rapidly with increasing φ. Furthermore, the overall behavior looks almost independent of the particle configurations. A theoretical model has been proposed by Levine and Neale for the electrophoretic mobility of dense dispersions by using the cell model [30]. They assumed the situation that a spherical particle with radius a is located at the center of a spherical container (cell) with radius b and calculated V as a function of κa and $\varphi = (a/b)^3$. Ohshima proposed a simpler expression for the mobility coefficient f according to the cell model [31]. Ohshima's prediction is shown in Fig. 3 (a) and (b) together with our numerical results. The overall agreement between our simulation and Ohshima's theory is better in (a) with a smaller Debye length $\kappa^{-1} = 5 = a$ than in (b) with a larger one $\kappa^{-1} = 10$. In both (a) and (b), the simulation results tend to be larger than the the theory as φ increases. We expect that the deviation is attributable to the occurrence of overlapping of the electric double layers for larger φ because such an effect is totally neglected in the theory. To this end, we estimated the effective radius $a + \kappa^{-1}$ of the ionically dressed particles and defined the effective volume fraction $\varphi_{eff} \equiv 4\pi(a + \kappa^{-1})^3N/3L^3 =$

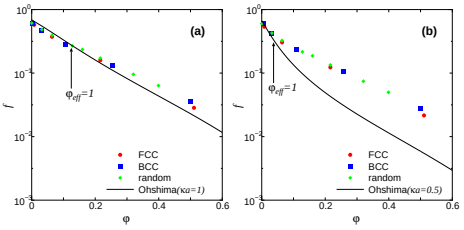

FIG. 3: The mobility coefficient $f(\kappa a, \varphi)$ as a function of the volume fraction φ in (a) $\kappa a = 1$ and (b) $\kappa a = 0.5$. The solid lines represent the approximation theory proposed by Ohshima [31]. The theory is confirmed to be accurate for $\varphi_{eff} \leq 1$, however, tends to deviate from our numerical results for $\varphi_{eff} > 1$ where overlapping of the electric double layers becomes notable.

$(1 + (\kappa a)^{-1})^3 \varphi$. As is clearly seen in Fig.3 (a) and (b), our results agree well with Ohshima' theory for $\varphi_{eff} \leq 1$ where the effect of overlapping is small. However, for $\varphi_{eff} > 1$ where the overlapping of the electric double layers becomes large, deviations between our simulations and the theory become notable. We emphasize that the present study is the first successful simulations which provide quantitative data necessary to examine the reliability of the Ohshima's cell model calculations including their boundary conditions for electrophoresis in dense colloidal dispersions. Our results are consistent with recent studies which also devoted to take into account the effects of double layer overlapping [19, 36, 37].

In summary, we have developed a unique numerical method for simulating electrohydrodynamic phenomena in colloidal dispersions. The method was first applied to simulate electrophoresis of a single spherical particle, and we found that our method can reproduce the reliable analytical theory proposed by O'Brien and White quantitatively. Simulations were then performed for electrophoresis of colloids in dense dispersions, and we compared them with the theoretical analysis based on the cell model. We found that the cell model is reliable when overlapping of electric double layers is small but less reliable as overlapping becomes larger.

[1] W. B. Russel, D. A. Saville, and W. R. Schowalter, *Colloidal Dispersions* (Cambridge University Press, Cambridge, 1989).
[2] J. F. Brady and G. Bossis, Ann. Rev. Fluid Mech. **20**, 111 (1988).
[3] H. H. Hu, N. A. Patankar, and M. Y. Zhu, J. Comput. Phys. **169**, 427 (2001).
[4] A. J. C. Ladd and R. Verberg, J. Stat. Phys. **104**, 1191 (2001).
[5] A. Malevanets and R. Kapral, J. Chem. Phys. **110**, 8605 (1999).
[6] H. Tanaka and T. Araki, Phys. Rev. Lett. **85**, 1338 (2000).
[7] T. Kajishima, S. Takiguchi, H. Hamasaki, and Y. Miyake, JSME Int. J. Ser. B **44**, 526 (2001).
[8] M. Fushiki, J. Chem. Phys. **97**, 6700 (1992).
[9] H. Löwen, P. A. Madden, and J.-P. Hansen, Phys. Rev. Lett. **68**, 1081 (1992).
[10] H. Löwen, J.-P. Hansen, and P. A. Madden, J. Chem. Phys. **98**, 3275 (1993).
[11] J. Chakrabarti, J. Dzubiella, and H. Löwen, Phys. Rev. E **70**, 012401 (2004).
[12] J. Dobnikar, Y. Chen, R. Rzehak, and H. H. von Grünberg, J. Chem. Phys. **119**, 4971 (2003).
[13] Y. W. Kim and R. R. Netz, Europhys. Lett. **72**, 837 (2005).
[14] T. Yamaue, M. Sasaki, and T. Taniguchi, Multi-Phase Dynamics Program "Muffin" User's Manual (2005), URL `http://octa.jp`.
[15] J. Horbach and D. Frenkel, Phys. Rev. E **64**, 061507 (2001).
[16] R. Z. Wang, H. P. Fang, Z. Lin, and S. Chen, Phys. Rev. E **68**, 011401 (2003).
[17] V. Lobaskin and B. Dünweg, J. Phys.: Condens. Matter **16**, S4063 (2004).
[18] A. Chatterji and J. Horbach, J. Chem. Phys **122**, 184903 (2005).
[19] V. Lobaskin, B. Dünweg, M. Medebach, T. Palberg, and C. Holm, cond-mat/0601588 (2006).
[20] H. Kodama, K. Takeshita, T. Araki, and H. Tanaka, J. Phys.: Condens. Matter **16**, L115 (2004).
[21] Y. Nakayama and R. Yamamoto, Phys. Rev. E **71**, 036707 (2005).
[22] Y. Nakayama, K. Kim, and R. Yamamoto, cond-mat/0601322 (2006).
[23] R. Yamamoto, Phys. Rev. Lett. **87**, 075502 (2001).
[24] R. Yamamoto, Y. Nakayama, and K. Kim, J. Phys.: Condens. Matter **16**, S1945 (2004).
[25] K. Kim and R. Yamamoto, Macromol. Theory Simul. **14**, 278 (2005).
[26] R. W. O'Brien and L. R. White, J. Chem. Soc. Faraday Trans. 2 **74**, 1607 (1978).
[27] M. von. Smoluchowski, Z. Phys. Chem. **92**, 129 (1918).
[28] E. Hückel, Phys. Z. **25**, 204 (1924).
[29] D. C. Henry, Proc. R. Soc. London Ser. A **133**, 106 (1931).
[30] S. Levine and G. H. Neale, J. Colloid Interface Sci. **47**, 520 (1974).
[31] H. Ohshima, J. Colloid Interface Sci. **188**, 481 (1997).
[32] J.-P. Hansen and H. Löwen, Annu. Rev. Phys. Chem. **51**, 209 (2000).
[33] J.-L. Barrat and J.-P. Hansen, *Basic Concepts for Simple and Complex Liquids* (Cambridge University Press, Cambridge, 2003).
[34] H. Ohshima, T. W. Healy, and L. R. White, J. Colloid Interface Sci. **90**, 17 (1982).
[35] See EPAPS Document No. [number will be inserted by publisher] for movies of FCC (Fig2a.mpg), BCC (Fig2b.mpg), and random (Fig2c.mpg) configurations. For more information on EPAPS, see http://www.aip.org/pubservs/epaps.html.
[36] F. Carrique, F. J. Arroyo, M. L. Jiménez, and Á. V. Delgado, J. Phys. Chem. B **107**, 3199 (2003).
[37] T. Palberg, M. Medebach, N. Garbow, M. Evers, A. B. Fontecha, H. Reiber, and E. Bartsch, J. Phys.: Condens. Matter **16**, S4039 (2004).